THE JOURNAL OF PHYSICAL CHEMISTRY C

Article

pubs.acs.org/JPCC

Modeling the Size-Dependent Solid−Solid Phase Transition Temperature of Cu_2S Nanosolids

Yejun Li,[†,‡] Weihong Qi,[†,*] Yuan Li,[†] Ewald Janssens,[‡] and Baiyun Huang[§]

[†]School of Materials Science and Engineering, Central South University, Changsha, 410083, China

[‡]Laboratory of Solid State Physics and Magnetism, Katholieke Universiteit Leuven, Celestijnenlaan 200 D, B-3001 Leuven, Belgium

[§]State Key Laboratory of Powder Metallurgy, Central South University, Changsha 410083, P.R. China

ABSTRACT: The present study provides a simple model to predict the favored phase of Cu_2S nanosolids upon variation of their size, shape, and temperature. Insight into the phase stability at the nanoscale will aid in the design of new nanomaterials. A study of the solid−solid phase transition demonstrated that the low-chalcocite to high-chalcocite transition temperature of Cu_2S nanowires increases with increasing wire diameter consistent with recent experimental data.[31] At ambient temperature, the high-chalcocite phase is the most stable phase for nanofilms with a thickness below 1.5 nm, nanowires with a diameter below 3 nm and nanoparticles smaller than 4.5 nm, all in agreement with experimental observations.

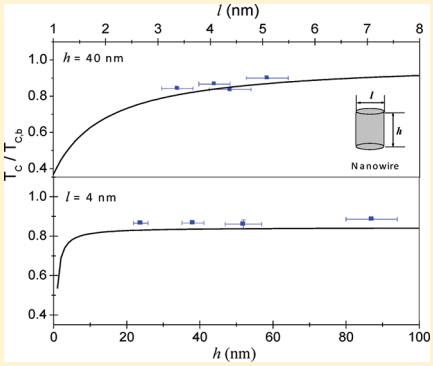

1. INTRODUCTION

Nanosolids have been considered in several recent applications due to their size dependent electronic, magnetic, optic, and catalytic properties. In addition, also the thermodynamic properties of nanosolids appear to be different from bulk materials.[1] It has been demonstrated experimentally that the melting temperature of metallic, semiconductor, organic as well as embedded nanoparticles depends on particle size.[2−5] The size dependence of their thermodynamic properties, i.e. cohesive energy, melting entropy, melting enthalpy and vacancy formation energy, has been studied theoretically.[6−10] The size dependent behavior was also shown to depend on the dimensions of the nanosolids.[7] One example is that the melting temperature variations of nanoparticles, nanofilms and nanowires of comparable size (diameters of nanoparticles and nanowires, thickness of nanofilms) follow the ratio 3:2:1.[10] These size effects are key to understand and design new functional nanomaterials.

Copper sulfide (Cu_2S), an indirect bandgap semiconductor,[11] has extensively been investigated and is widely used in solar cells,[12] field emission,[13] switching,[14] and sensing devices.[15] Several recent studies have demonstrated that understanding the role of size effects on the phase stability and the phase transition temperature is crucial before Cu_2S nanosolids based devices can be developed.[16−28] Stoichiometric Cu_2S exhibits a low-chalcocite phase (LC) at room temperature and transforms to high-chalcocite (HC) at 376.65 K.[29] During this transition, the sulfur atoms almost maintain their original positions, whereas the copper atoms obtain a disordered distribution compared to the LC lattice sites. In other words, the LC→HC transition can be regarded as an order−disorder transition. The structure of LC leads to an indirect bandgap of ∼1.2 eV, whereas the HC phase shows a reduced mobility (for holes and electrons) and has an increased indirect bandgap of ∼1.42 eV.[11] The phase transition in Cu_2S also has been studied in nanosolids.[16−28,30,31] Liu et al.[16] and Korgel et al.[18,19] have shown that HC nanoparticles (NPs) can exist at low temperature indicating a size dependent phase stability of Cu_2S NPs. Recently, Zheng et al. studied the dynamics of the LC→HC phase transition in Cu_2S nanowires (NWs) by visualizing structural fluctuations during the transition process.[30] Rivest and co-workers measured the transition temperature (T_C) of Cu_2S NWs with different diameters and found that the T_C of Cu_2S NWs was substantially lower than the bulk value, with a maximum depression of 60 K.[31] They also found that the T_C is sensitive to the wire diameter but insensitive to the wire length. Whereas these are interesting and significant experimental results, there is no theoretical model available to explain them. In this letter, we present a simple model to account for the size dependent LC→HC transition temperature of Cu_2S nanosolids aiming to explain the recent experimental findings and to provide crucial insight into the relative phase stability and the transition mechanism at the nanoscale.

2. MODEL

A solid−solid phase transition can be studied by considering the free energy of the different phases. The free energy difference ΔG between HC and LC at a specified temperature T and pressure P can be written as

Received: January 11, 2012
Revised: March 24, 2012

   dx.doi.org/10.1021/jp3003307 | J. Phys. Chem. C XXXX, XXX, XXX−XXX

$$\Delta G = \Delta E + P\Delta V - T\Delta S \quad (1)$$

where $\Delta E = E_{HC} - E_{LC}$ with E_{HC} and E_{LC} the cohesive energy (CE) of HC and LC, respectively. $\Delta S = S_{HC} - S_{LC}$ and $\Delta V = V_{HC} - V_{LC}$ are the corresponding entropy and volume changes during the phase transition. For $\Delta G > 0$ LC is stable, and for $\Delta G < 0$ HC is stable, whereas $\Delta G = 0$ can be used to determine the LC→HC transition temperature.

The CE of a nanosolid can be computed by the Generalized−Bond−Energy (GBE) model,[32] where the nanosolid can be regarded as in core−shell structure and its cohesive energy is the sum of contributions from both the shell and core atoms. If only the face atoms are considered, the corresponding formulas of the CE per atom of the nanosolid E_p is $E_p = E_b[1 - (1/N)\Sigma_i S_i \rho_i (1 - A_i)]$, where E_b is the cohesive energy per atom of the bulk material and N is the total number of atoms. In general, a nanosolid is enclosed by several face planes. For the ith plane, the surface area is S_i and the corresponding atom density is ρ_i. The parameter A_i is the ratio between the total number of bonds of a surface atom in the ith plane and the total number of bonds of a core atom. We assume all Cu−Cu (or Cu−S) bonds are the same in LC and HC, and that parameters S_i, ρ_i, and A_i are invariant during LC→HC transition. We have not found any reports on surface reconstruction of Cu_2S NWs from literatures, and for simplicity, the surface reconstruction has been neglected. And then the CE difference of the nanosolid between LC and HC is

$$\Delta E = E_{p,HC} - E_{p,LC} = \Delta E_b[1 - (1/N)\sum_i S_i\rho_i(1 - A_i)] \quad (2)$$

where $\Delta E_b = E_{b,HC} - E_{b,LC}$ is the CE difference between bulk LC and HC.

The volumes of different phases in Cu_2S can be calculated using the lattice parameters provided by the Joint Committee on Power Diffraction Standards (JCPDS). Because the lattice contraction due to size reduction is 1% or smaller,[33] we assume that the Cu_2S nanosolids have the same lattice structure as the bulk material and ignore the volume variation. Indeed, at atmospheric pressure, $P\Delta V$ corresponds to 5.33×10^{-8}eV for the LC→HC transition (the value is calculated from the JCPDS standard 00−033−0490 (LC) and the JCPDS standard 00−046−1195 (HC)), which is about 10^{-8} times smaller than the CE. The effect of the volume variation on the free energy thus can be ignored.

The last term in eq 1 is related to the entropy change during the phase transition. The entropy consists of the electronic entropy S_{elec}, the configurational entropy S_{conf}, and the vibrational entropy S_{vib}. Therefore, $\Delta S = \Delta S_{elec} + \Delta S_{conf} + \Delta S_{vib}$. According to either the Einstein or Debye specific heat model,[34] the contribution of S_{elec} to the total entropy at temperatures relevant for the LC→HC phase transition is very small and can be ignored. Since the positions of the Cu and S atoms in Cu_2S NPs are almost unchanged compared to bulk Cu_2S,[31] $\Delta S_{conf} = S_{conf,HC} - S_{conf,LC}$ of the NP equals the bulk value. In the bulk, the atomic vibrational entropy difference can be computed as $\Delta S_{b,vib} = S_{vib,HC} - S_{vib,LC} = 3Nk_B \ln(\theta_{b,LC}/\theta_{b,HC})$, where k_B is the Boltzmann constant, $\theta_{b,LC}$ and $\theta_{b,HC}$ are the Debye temperatures of LC and HC solids. This equation was derived by Anthony et al. under the assumption that the ratio of the vibrational frequencies of the disordered alloy to those of the ordered alloy is the same for all modes.[35] For nanosolids, the vibrational entropy difference becomes $\Delta S_{p,vib} = 3Nk_B \ln(\theta_{p,LC}/\theta_{p,HC})$, with Debye temperatures $\theta_{p,LC}$ and $\theta_{p,HC}$ for the LC and HC nanosolids. Because the Debye temperature follows the size dependence of the cohesive energy,[36] one finds $\theta_{p,LC}/\theta_{p,HC} = \theta_{b,LC}/\theta_{b,HC}$ and thus $\Delta S_{p,vib}=\Delta S_{b,vib}$. Although the vibrational entropy depends on the size of nanosolids, the vibrational entropy difference between HC and LC is size-independent. In summary, the entropy difference during the phase transition does not depend on the size of the nanosolids, that is $\Delta S = \Delta S_b$.

Then the free energy difference between the two phases of the nanosolid is:

$$\Delta G = \Delta E_b[1 - (1/N)\sum_i S_i\rho_i(1 - A_i)] - T\Delta S_b \quad (3)$$

At the LC→HC T_C, corresponding to $\Delta G = 0$, equals:

$$T_C = T_{C,b}[1 - (1/N)\sum_i S_i\rho_i(1 - A_i)] \quad (4)$$

where $T_{C,b} = \Delta E_b/\Delta S_b$, corresponding to $N\to\infty$, can be regarded as the bulk LC→HC transition temperature.

Eq 4 indicates that the T_C of a nanosolid depends on the term $(1/N)\sum_i S_i\rho_i(1 - A_i)$. For simplicity, we assume all facets of the nanosolid have the identical atomic density, and $A_i = {}^1/_4$ after considering surface relaxation.[37] Eq 4 can be simplified to the following form for a regular polyhedral NP:

$$T_C = T_{C,b}\cdot(1 - 3\alpha d/D) \quad (5)$$

with d and D, the atomic diameter and NP diameter, respectively. The parameter α, that is, shape factor, defined as the surface area ratio between a nonspherical NP and a spherical one with identical volume, is introduced to describe the shape effect.[37] For a disk-like NP with diameter l and length h, eq 4 can be simplified to:

$$T_C = T_{C,b}[1 - d(2/l + 1/h)] \quad (6)$$

If $h\to\infty$, the disklike NP becomes a NW. For $l\to\infty$, the disk-like NP can be considered as a nanofilm (i.e., NF). For both LC and HC Cu_2S, the atomic density is 5.6 g/cm^3,[38] which corresponds to $d = 0.313$ nm. In the following, we will use eqs 5 and 6 to compare our model with several recent experiments.

3. RESULTS AND DISCUSSION

Figure 1 depicts the size dependence of the LC→HC T_C of Cu_2S NWs with respect to the bulk $T_{C,b} = 376.65$ K. The solid line is the calculated result and experimental data points are shown as a circle,[21] a triangle,[30] and squares,[31] respectively. T_C increases with increasing diameter l and approaches $T_{C,b}$ as $l \to \infty$, which shows that the T_C reduction for NWs is a surface-dominated effect induced by the strongly increased surface-to-volume atomic ratio. Although the model prediction is, given the experimental uncertainty and the model assumptions, in good agreement with the experimental data, it slightly underestimates the experimental results. In present calculation, the value of A_i equals ${}^1/_4$, as in metallic nanomaterials, which may be low for Cu_2S NWs, and leads to the underestimation. According to eq 3, it is interesting to find that the free energy difference around the transition point decrease as the size decreases, which may also explain the broadening of the transition region of Cu_2S NWs in the experiment of Zhang et al.[30] In general, energy fluctuations exist around the transition point. When those fluctuations are larger than the energy barrier between the two phases, the transition from one phase to the other happens. The reduction of the free energy

dx.doi.org/10.1021/jp3003307 | J. Phys. Chem. C XXXX, XXX, XXX−XXX

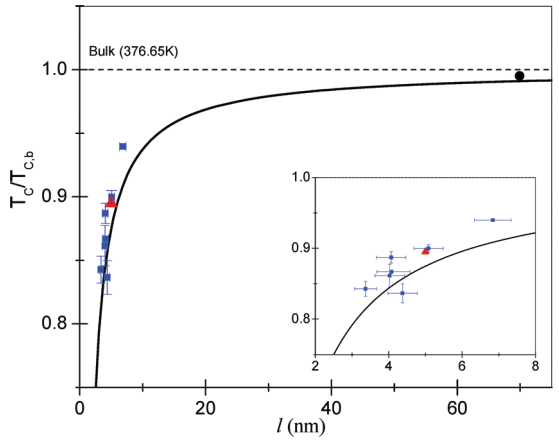

Figure 1. Dependence of the LC→HC T_C in Cu_2S NWs as a function of the NW diameter. The solid line represents the present calculated results; experimental data points are shown as '●',[21] '▲',[30] and '■'[31] symbols. The insert gives a magnified view for small NW diameters.

difference in small NWs means a lower energy barrier, which will result in a larger transition region. This also explains why the transition region of larger NWs is much sharper than the transition region of small NW in the experiments of Rivest et al.[31]

The length and diameter dependences of the LC→HC T_C of Cu_2S NWs are plotted in Figure 2. The experimental data for

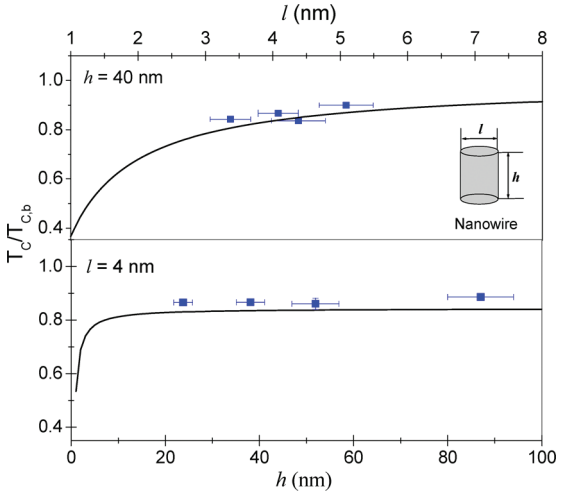

Figure 2. Diameter l and length h dependence of the LC→HC T_C in Cu_2S NWs for h = 40 nm (upper panel) and l = 4 nm (lower panel). The solid lines represent the calculated results and '■'[31] symbols the experimental data. The insert shows a schematic diagram of NWs.

NWs with l = 4 nm and h = 40 nm, as obtained by Rivest et al,[31] are added for comparisons. The upper panel shows a strong diameter dependence of T_C, consistent with the experimental data. The lower panel, however, shows discrepancies between the experimental data points and the model for the length dependence of T_C. This may result from the diameter deviation of the experimental NWs.[31] A 10% variation of the diameter from 3.6 to 4.4 nm will result in a significant change in T_C as shown in Figure 1. T_C is almost constant for h > 20 nm (T_C increases only 4.5 K from h = 20 nm to h = 80 nm), whereas a rapid reduction is found for small h (especially if h < 15 nm). Because one cannot speak about NWs if h becomes comparable to l, it is safe to say that the NW length has no significant effect on T_C. A mimic behavior is found for NFs (not on figure): the T_C of NFs depends strongly on film thickness but is less sensitive to the lateral dimensions as long as these are much larger than the thickness.

Figure 3 compares the LC→HC T_C of Cu_2S nanosolids with different dimensions. For as well NPs, as NWs and NFs, T_C

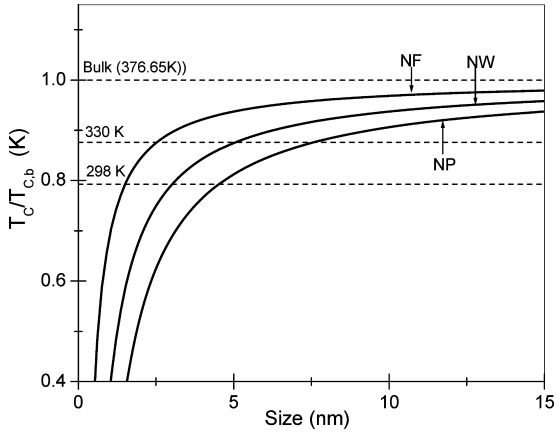

Figure 3. Dimension dependence of the LC→HC T_C in Cu_2S nanosolids. The solid lines represent the calculated results for spherical NPs, cylindrical NWs and NFs, respectively.

decreases with decreasing size. However, the depression of T_C is strongly dimension dependent and follows for spherical NPs, cylindrical NWs and NFs at the same characteristic sizes: $(\Delta T_{C,NP}/\Delta T_{C,b}):(\Delta T_{C,NW}/\Delta T_{C,b}):(\Delta T_{C,NF}/\Delta T_{C,b})$ = 3:2:1, like several other thermodynamic properties at the nanoscale.[39]

Upon tuning the T_C of Cu_2S nanosolids by nanostructuring, certain properties may be favored, which renders controlling T_C of importance for applications. For example, at the photovoltaic operating temperature ($T_{operate}$ = 300−330 K), a deleterious phase (HC) should be avoided. To retain the LC phase at $T_{operate}$, it is necessary to produce nanosolids with a characteristic size larger than 2.5 nm for h of NFs, 5.1 nm for l of NWs, and 7.5 nm for D of NPs (Figure 3). The calculated critical size (5.1 nm) for NWs is consistent with the experimental prediction (6 nm).[31]

At ambient temperature, a lot of experiments have shown that some synthesized Cu_2S nanosolids have HC phase, whereas others, with typically a larger size, take the LC phase. This suggests that the LC phase is relatively less stable when the size of nanosolids is reduced.[16−28] Though an exact value for the ambient temperature is not given in all references and some experiments may have been carried out at slightly higher temperature, we here assume $T_{ambient}$ = 298 K for all experimental work carried out at ambient temperature. As shown in Figure 3, our model predicts the HC phase at $T_{ambient}$ when synthesized nanosolids are smaller than a critical size of 1.5 nm for h of NFs, 3 nm for l of NWs, and 4.5 nm for D of NPs. The critical diameter for NWs (3 nm) is close to the prediction by Rivest et al (2.5 nm).[31] In other words, if the T_C of those nanosolids is lower than $T_{ambient}$, the HC phase is stable.

Table 1 compares the available experimental results and our model prediction for the phase stability of Cu_2S nanosolids at ambient temperature. Agreement is found with all available studies, that is, refs 16, 17, 20−25, 27, 28, except with the work presented in refs 18, 19, 26.

dx.doi.org/10.1021/jp3003307 | J. Phys. Chem. C XXXX, XXX, XXX−XXX

Table 1. Phase Stability of Cu_2S Nanosolids at Ambient Temperature, the T_C is Calculated with the Present Model for the Geometry of the Nanosolids in the Experiment, the Modeled T_C Is Then Used to Compare the Experimentally Observed Phase with the Model Prediction

	size	modeled T_C	experimental results	model predictions
NWs	l = 2.5 nm[16]		HC[16]	HC
	l = 10−80 nm[20−24]		LC[20−24]	LC
NFs	h = 70 nm[28]		LC[28]	LC
NPs	D = 4 nm[17]		HC[17]	HC
	D = 5.4 nm[25]	296 K	HC[25]	HC
Disk-like NPs	l = 8.9 nm h = 2 nm[17]	290 K	HC[17]	HC
	l = 4 nm h = 12 nm[18]	307 K	HC[18]	LC
	l = 3−150 nm h = 3 −12 nm[19]	259−340 K	HC[19]	LC and HC
	l = 9 nm h = 4.5 nm[26]	323 K	HC[26]	LC
	l = 6 nm h = 48 nm[27]	334 K	LC[27]	LC
	l = 9 nm h = 29 nm[27]	346 K	LC[27]	LC

For the Cu_2S NPs with D = 5.4 nm,[25] a LC phase should be expected according to Figure 3. However, taking into account the hexagonal-faceted shape of the NPs in ref 25, a shape factor α = 1.20 has to be applied, yielding a modeled transition temperature of T_C = 296 K. This is slightly below $T_{ambient}$ in agreement with the experiment result. A similar remark has to be made for the disklike NPs in ref 18. Those disk-like Cu_2S NPs have a shape distribution in the experiment, whereas they are considered to be cylindrical in the present calculation. This may increase the actual surface-to-volume atomic ratio and bring T_C below $T_{ambient}$. It should be mentioned that the Cu_2S NPs have a triangular shape (side length 12 nm and h = 2 nm) in ref 17, which equals to the disklike NPs with diameter l = 8.9 nm and h = 2 nm by identical area conversion. As mentioned above, the actual temperature of the experiments may deviate from $T_{ambient}$ = 298 K. A higher real temperature may be the reason for the observation of the HC phase for Cu_2S nanosolids with larger size found in other experiments.[19] Nevertheless, the agreement between the experiment observations and the model prediction confirms the efficiency of the present model.

For bulk materials, Cu_2S will take a cubic phase (CB) when the temperature increases above $T_{C,b}$ = 711 K.[40] Though there is no experimental report yet on the HC→CB phase transition in Cu_2S nanosolids, assuming the T_C of this transition has the same size dependent behavior, a further calculation by the present theory shows that CB phase in Cu_2S NWs may be expected at $T_{ambient}$ when l < 1.1 nm. The experimental difficulty to synthesize Cu_2S NWs with such small diameters may be the reason that this phase transition is not discovered yet. It should also be noted that small particles containing less than a few tens of atoms, may be amorphous and the statistic meaning is no longer valid.[39] Their structural stability and properties are sensitive to the number of total atoms, and quantum size effects may dominate the properties of particles smaller than 1 nm. The present model is a semiempirical model and cannot be extrapolated to subnanometer particles. Therefore, the discussion of small nanosolids is out of its scope. Nevertheless, the above discussions provide us insight in possible access to favored phase in nanomaterials with special properties by controlling the size, shape, and temperature.

4. CONCLUSIONS

In this work, the size dependence of solid−solid phase transition of Cu_2S nanosolids is investigated. A lowering of T_C is found when reducing the size of the nanosolids, which is consistent with experimental results available in literature. The magnitude of the reduction of T_C is dimension dependent and follows the ratios 3:2:1 for spherical NPs, cylindrical NWs and NFs at the same size. The reduction of T_C allows to synthesize phases in Cu_2S nanosolids that are not found in bulk material under ambient conditions. In particular the HC phase is obtained for nanosolids with sizes smaller than the critical size, that is 1.5, 3, and 4.5 nm for h of NFs, l of NWs and D of NPs. The model predictions are confirmed by the experimental observations. Moreover, the CB phase in Cu_2S NWs may be expected when the diameter is below 1.1 nm. We believe that the present study provides a simple model to predict the favored phase in Cu_2S nanosolids upon variation of their size, shape, and temperature, and gives insight into the phase stability and transition mechanisms at the nanoscale.

AUTHOR INFORMATION

Corresponding Author

*E-mail: qiwh216@mail.csu.edu.cn (W.H.Qi).

Notes

The authors declare no competing financial interest.

ACKNOWLEDGMENTS

This work was supported by Program for New Century Excellent Talents in University (No. NCET-08-0574), Hunan Provincial Natural Science Foundation of China (No. 09JJ3106), Fund for Scientific Research − Flanders (FWO), the KU Leuven Research Council (GOA), Shenghua Scholar Program of Central South University and Aid program for Science and Technology Innovative Research Team in Higher Educational Institutions of Hunan Province.

REFERENCES

(1) Gleiter, H. Nanostructured materials: Basic concepts and microstructure. *Acta Mater.* **2000**, *48*, 1−29.
(2) Chattopadhyuy, K.; Goswami, R. Melting and superheating of metals and alloys. *Prog. Mater. Sci.* **1991**, *42*, 287−300.
(3) Goldstein, A. N. The melting of silicon nanocrystals: Submicron thin-film structures derived from nanocrystal precursors. *Appl. Phys. A: Mater. Sci. Process.* **1996**, *62*, 33−37.
(4) Morishige, K.; Kawano, K. Freezing and melting of methyl chloride in a single cylindrical pore: anomalous pore-size dependence of phase-transition temperature. *J. Phys. Chem. B* **1999**, *103*, 7906−7910.
(5) Sheng, H. W.; Ren, G.; Peng, L. M.; Hu, Z. Q.; Lu, K. Epitaxial dependence of the melting behavior of In nanoparticles embedded in Al matrices. *J. Mater. Res.* **1997**, *12*, 119−123.
(6) Jiang, Q.; Aya, N.; Shi, F. G. Nanotube size-dependent melting of single crystals in carbon nanotubes. *Appl. Phys. A: Mater. Sci. Process.* **1997**, *64*, 627−629.
(7) Qi, W. H.; Wang, M. P.; Zhou, M.; Hu, W. Y. Surface-area-difference model for thermodynamic properties of metallic nanocrystals. *J. Phys. D: Appl. Phys* **2005**, *38*, 1429−1436.
(8) Qi, W. H.; Wang, M. P. Size dependence of vacancy formation energy of metallic nanoparticles. *Physica B* **2003**, *334*, 432−435.

(9) Qi, W. H.; Wang, M. P.; Xu, G. Y. The particle size dependence of cohesive energy of metallic nanoparticles. *Chem. Phys. Lett.* **2003**, *372*, 632−634.
(10) Ruffino, F.; Grimaldi, M. G.; Giannazzo, F.; Roccaforte, F.; Raineri, V. Thermodynamic properties of supported and embedded metallic nanocrystals: gold on/in SiO_2. *Nanoscale Res. Lett.* **2008**, *3*, 454−460.
(11) Xu, N. S.; Huq, S. E. Novel cold cathode materials and applications. *Mater. Sci. Eng. R* **2005**, *48*, 47−189.
(12) Neville, R. C. *Solar energy conversion: The solar cell*, 2nd ed.; Elsevier: Amsterdam, 1995.
(13) Feng, X. P.; Li, Y. X.; Liu, H. B.; Li, Y. L.; Cui, S.; Wang, N.; Jiang, L.; Liu, X. F.; Yuan, M. J. Controlled growth and field emission properties of CuS nanowalls. *Nanotechnology* **2007**, *18*, 145706.
(14) Sakamoto, T.; Sunamura, H.; Kawaura, H.; Hasegawa, T.; Nakayama, T.; Aono, M. Nanometer-scale switches using copper sulfide. *Appl. Phys. Lett.* **2003**, *82*, 3032−3034.
(15) Sagade, A. Copper sulphide (Cu_xS) as an ammonia gas sensor working at room temperature. *Sens. Actuators B* **2008**, *133*, 135−143.
(16) Liu, Z. P.; Xu, D.; Liang, J. B.; Shen, J. M; Zhang, S. Y.; Qian, Y. T. Growth of CuS ultrathin nanowires in a binary surfactant solvent. *J. Phys. Chem. B* **2005**, *109*, 10699−10704.
(17) Lee, H.; Yoon, S. W.; Kim, E. J.; Park, J. In-situ growth of copper sulfide nanocrystals on multiwalled carbon nanotubes and their application as novel solar cell and amperometric glucose sensor materials. *Nano Lett.* **2007**, *7*, 778−784.
(18) Larsen, T. H.; Sigman, M.; Ghezelbash, A.; Doty, R. C.; Korgel, B. A. Solventless synthesis of copper sulfide nanorods by thermolysis of a single source thiolate-derived precursor. *J. Am. Chem. Soc.* **2003**, *125*, 5638−5639.
(19) Sigman, M. B.; Ghezelbash, J. A.; Hanrath, T.; Saunders, A. E.; Lee, F.; Korgel, B. A. Solventless synthesis of monodisperse Cu_2S nanorods, nanodisks, and nanoplatelets. *J. Am. Chem. Soc.* **2003**, *125*, 16050−16057.
(20) Wang, S. H.; Yang, S. H.; Dai, Z. R.; Wang, Z. L. The crystal structure and growth direction of nanowire arrays Cu_2S fabricated on a copper surface. *Phys. Chem. Chem. Phys.* **2001**, *3*, 3750−3753.
(21) Wang, S. H.; Yang, S. H. Growth of crystalline Cu_2S nanowire arrays on copper surface: effect of copper surface structure, reagent gas composition, and reaction temperature. *Chem. Mater.* **2001**, *13*, 4794−4799.
(22) Wang, S. H.; Guo, L.; Wen, X. G.; Yang, S. H.; Zhao, J.; Liu, J.; Wu, Z. H. Phase transitions in the Cu_2S nanowires. *Mater. Chem. Phys.* **2002**, *75*, 32−38.
(23) Zhao, S. H.; Han, G. Y.; Li, M. Y. Fabrication of copper sulfide microstructures with the bottle- and thorny rod-shape. *Mater. Chem. Phys.* **2010**, *120*, 431−437.
(24) Lai, C. X.; Wu, Q. B.; Chen, J.; Wen, L. S.; Ren, S. Large-area aligned branched Cu2S nanostructure arrays: room-temperature synthesis and growth mechanism. *Nanotechnology* **2010**, *21*, 215602 (5pp).
(25) Wu, Y.; Wadia, C.; Ma, W.; Sadtler, B.; Alivisatos, A. P. Synthesis and photovoltaic application of copper (I) sulfide nanocrystals. *Nano Lett.* **2008**, *8*, 2551−2555.
(26) Zhang, H. T.; Wu, G.; Chen, X. H. Large-Scale synthesis and self-assembly of monodisperse hexagon Cu_2S nanoplates. *Langmuir* **2005**, *21*, 4281−4282.
(27) Sadtler, B.; Demchenko, D. O.; Zheng, H. M.; Hughes, S. M.; Merkle, M. G.; Dahmen, U.; Wang, L. W.; Alivisatos, A. P. Selective facet reactivity during cation exchange in cadmium sulfide nanorods. *J. Am. Chem. Soc.* **2009**, *131*, 5285−5293.
(28) Ubalea, A. U.; Choudhari, D. M.; Kantale, J. S.; Mitkari, V. N.; Nikam, M. S.; Gawande, W. J.; Patil, P. P. Synthesis of nanostructured Cu_xS thin films by chemical route at room temperature and investigation of their size dependent physical properties. *J. Alloys Compd.* **2011**, *509*, 9249−9254.
(29) Sands, T. D.; Washburn, J.; Gronsky, R. High resolution observations of copper vacancy ordering in chalcocite (Cu_2S) and the transformation to djurleite ($Cu_{1.97\ to\ 1.94}S$). *Phys. Status Solidi A* **1982**, *72*, 551−559.
(30) Zheng, H. M.; Rivest, J. B.; Miller, T. A.; Sadtler, B.; Lindenberg, A.; Toney, M. F.; Wang, L. W.; Kisielowski, C.; Alivisatos, A. P. Observation of transient structural-transformation dynamics in a Cu_2S nanorod. *Science* **2011**, *333*, 206−209.
(31) Rivest, J. B.; Fong, L. K.; Jain, P. K.; Toney, M. F.; Alivisatos, A. P. Size dependence of a temperature-induced solid-solid phase transition in copper(I) sulfide. *J. Phys. Chem. Lett.* **2011**, *2*, 2402−2406.
(32) Qi, W. H.; Huang, B. Y.; Wang, M. P.; Li, Z.; Yu, Z. M. Generalized Bond-Energy model for cohesive energy of small metallic particles. *Phys. Lett. A* **2007**, *370*, 494−498.
(33) Qi, W. H.; Wang, M. P. Size and shape dependent lattice parameters of metallic nanoparticles. *J. Nanopart. Res.* **2005**, *7*, 51−57.
(34) Landau, L. A.; Lifshitz, E. M. *Statistical Physics*; Pergamon Press: Oxford, 1958.
(35) Anthony, L.; Okamoto, K.; Fultz, B. Vibrational entropy of ordered and disordered Ni_3Al. *Phys. Rev. Lett.* **1993**, *70*, 1128−1130.
(36) Xiong, S. Y.; Qi, W. H.; Huang, B. Y.; Wang, M. P.; Wei, L. Y. Gibbs free energy and size-temperature phase diagram of hafnium nanoparticles. *J. Phys. Chem. C* **2011**, *115*, 10365−10369.
(37) Qi, W. H.; Wang, M. P. Size and shape dependent melting temperature of metallic nanoparticles. *Mater. Chem. Phys.* **2004**, *88*, 280−284.
(38) Buerger, M. J.; Buerger, N. W. Low-chalcocite and high-chalcocite. *Am. Mineral.* **1944**, *29*, 55−65.
(39) Nanda, K. K.; Sahu, S. N.; Behera, S. N. Liquid-drop model for the size-dependent melting of low-dimensional systems. *Phys. Rev. A* **2002**, *66*, 013208−013215.
(40) Potter, R. W. An electrochemical investigation of the system copper-sulfur. *Econ. Geol.* **1977**, *72*, 1524−1542.

dx.doi.org/10.1021/jp3003307 | *J. Phys. Chem. C* XXXX, XXX, XXX−XXX